Electronic structure of Li-intercalated oligopyridines: A comparative study by photoelectron spectroscopy

Walter J. Doherty III[a] and Rainer Friedlein[b]
Department of Physics, Chemistry, and Biology (IFM), Linköping University, 581 83 Linköping, Sweden

Thierry Renouard[c] and Claude Mathis
Institut Charles Sadron, UPR 22-CNRS, 6 Rue Boussingault, 67083 Strasbourg Cedex, France

William R. Salaneck
Department of Physics, Chemistry, and Biology (IFM), Linköping University, 581 83 Linköping, Sweden

(Received 13 July 2006; accepted 23 January 2007; published online 7 March 2007)

The role of nitrogen in the charge transfer and storage capacity of lithium-intercalated heterocyclic oligophenylenes was investigated using photoelectron spectroscopy. The development of new occupied states at low binding energies in the valence band region, as well as core level chemical shifts at both carbon and nitrogen sites, demonstrates partial charge transfer from lithium atoms to the organic component during formation of the intercalated compound. In small compounds, i.e., biphenyl and bipyridine derivatives, the position of the nitrogen heteroatom significantly affects the spacing between gap states in the Li-intercalated film; yet it has minimal effects on the charge storage capacity. In larger, branched systems, the presence of nitrogen in the aromatic system significantly enhances the charge storage capacity while the Li–N bond strength at high intercalation levels is significantly weakened relative to the nitrogen-free derivative. These observations have strong implications towards improved deintercalation processes in organic electrodes in lithium-ion batteries. © *2007 American Institute of Physics*. [DOI: 10.1063/1.2710262]

INTRODUCTION

Strong efforts within the electronics industry are focused on the development of organic transistor and display technologies due to the benefits inherent to organic electronics: lightweight applications, flexibility (both physical and chemical), and inexpensive processing. To take full advantage of these technologies it is necessary that the power supply also exhibits these same benefits. Batteries consisting of a lithium-intercalated, carbon-based electrode have the potential to meet these requirements. In these applications, lithium is the preferred active element since it is small and lightweight, allowing fast ionic conduction into intermolecular space, and exhibits a high gravimetric charge density with low electronegativity. Efficacy in lithium-based rechargeable batteries is determined by the capacity and reversibility of charge storage in the carbon-based matrix.

The intercalation of lithium into carbon-based materials shows considerable dependence on both the local structure and the microscopic aggregation state of the material. A doubling of charge storage capacity, as evidenced by current density measurements, was observed for disordered carbon versus crystalline graphite[1] and for opened versus closed single-wall carbon nanotubes.[2] It is postulated that these differences arise from the mechanisms through which lithium binds to the organic matrix, and several theoretical studies that describe the energetics of lithium binding sites in graphitic materials have been reported.[3–8]

Alternatively, it should be considered that the charge storage ability of an aromatic or conjugated π electronic system depends on the size and chemical structure of the molecule itself. It was noted that less energy is required to add charge to a small molecule versus a larger analog in terms of charge storage per carbon atom.[9] However, the energetics of lithium intercalation in carbon-based or organic matrices is not properly described by molecular properties[9] alone. The Madelung energy, the molecular electron affinity, and the Li ionization potential at particular bonding sites within the lattice must also be considered.[9,10] Additionally, these parameters are screened by electronic polarization.[11] Polarization energy varies as a function of aggregation state within a material and has been observed to ultimately determine the charge storage capabilities in thin films of α- versus β-perylene.[11]

Charge transfer into π-conjugated or aromatic systems usually results in the emergence of electronic states in the band gap of the pristine material resulting from the injection of charge into the lowest unoccupied molecular orbital (LUMO) and a destabilization of the highest occupied molecular orbital (HOMO) of the organic material.[12,13] For polymers or oligomeric materials with nondegenerate ground states, such charge-transfer states are termed polarons (singly charged) or bipolarons (doubly charged), where a bipolaron can be represented as an energetically favorable interaction

[a]Author to whom correspondence should be addressed. Present address: Chemical and Biosciences Center, National Renewable Energy Laboratory (NREL), 1617 Cole Boulevard, Golden, Colorado 80401; Tel: (303) 384-6775: Fax: (303) 384-6655; electronic mail: walter_doherty@nrel.gov
[b]Present address: School of Materials Science, Japan Advanced Institute of Science and Technology, 1-1 Asahidai, Nomi, Ishikawa 923-1292, Japan.
[c]Present address: UMR CNRS 6226 Equipe Chimie et Ingénierie des Procédés (CIP), Université de Rennes 1, 263 Avenue du Général Leclerc, CS 74205, 35042 Rennes Cedex, France.

between two neighboring polarons.[14,15] These charged sites are strongly stabilized and localized by the presence of counterions and coupled to local lattice deformations which can result in a structural change from an aromatic to a quinoidal system.[16–18] In alkali-intercalated polymers, *ab initio* calculations have shown that the charge transfer and defect sites are localized on the same monomer unit as the alkali atom,[19,20] allowing the use of small oligomeric systems as representative of the polymer.

The incorporation of heteroatoms, particularly nitrogen, into organic matrices has been considered as a means to produce novel materials with improved charge and energy storage characteristics in organic batteries. Several reports on nitrogen-substituted organic materials indicate an increase in charge storage capacity[21] and/or reversibility[22–24] relative to pure carbon-based systems. Conversely, molecular orbital calculations by Ago *et al.*[3] and electrochemical studies by Weydanz *et al.*[25] predict no real benefit to charge storage and a decrease in reversibility. These results are contradictive, suggesting that the charge storage properties may depend more on the bonding configuration of the heteroatom than the structural properties of the material. Recent studies on oligoanilines[26] have demonstrated that the charge transfer from lithium is largely localized at nitrogen atomic sites. In addition, theoretical calculations on systems in which nitrogen is substituted within an aromatic ring,[27–29] or a graphitic plane,[30] show that the most energetically favorable binding site for lithium directly involves the heteroatom.

This work serves as a systematic study of lithium intercalation in nitrogen heteroatomic, organic materials using photoelectron spectroscopy. The study extends from biphenyl and small model bipyridine compounds to larger, branched oligomeric systems. The electronic states of the materials were probed before and after lithium intercalation in order to elucidate the role of the heteroatom, its bonding configuration, and the size of the molecular π electronic system in the energy and charge storage properties of lithium-hetero-organic networks.

EXPERIMENTAL AND CALCULATIONS

Biphenyl (BP), 2,2′-bipyridyl (2bipy), 4,4′-bipyridyl (4bipy), and 2,2′-bipyrimidyl (2bpmy) were obtained from Aldrich (purity $\geqslant$ 99%) and used without further purification. 1,2,4,5-tetraphenylbenzene (TPB) and 2,3,5,6-tetrakis(2′-pyridyl)pyrazine (TPP) were synthesized according to Berthiol *et al.*[31] and Goodwin and Lions,[32] respectively. TPB and TPP were purified once by vacuum sublimation before use. Thin films of these materials were vapor deposited onto polycrystalline Cu substrates which were sputtered *in vacuo* by Ne^+ bombardment followed by annealing at 570 K. The deposition was carried out at a base pressure of less than 1×10^{-9} mbar. Molecules were contained approximately 5 cm from the sample in a glass crucible and degassed at 340 K for 5 min *prior* to film deposition. Films were prepared on substrates held at temperatures of 77 K for the smaller molecular weight materials and at 295 K for TPB and TPP. The crucible temperature used during deposition varied between samples: 340 K for BP, 350 K for 2bipy, 400 K for 4bipy, 370 K for 2bpmy, 580 K for TPB, and 600 K for TPP. Film thickness was controlled by deposition time (1–5 min) and deemed appropriate upon near-complete suppression of the Cu(L_3VV) Auger line from the underlying substrate, indicating an approximate film thickness of 3 nm. Intercalation of lithium was carried out by exposure of the pristine organic film to a vapor of Li atoms. Li was dosed in precalibrated amounts from an outgassed SAES getter source.

The intercalation was followed *in situ* by x-ray photoelectron spectroscopy (XPS) and ultraviolet photoelectron spectroscopy (UPS). Measurements were carried out using an instrument designed and built in our laboratory.[33] XPS spectra were obtained using an unfiltered Al $K\alpha$ x-ray source (1486.6 eV) with an energy analyzer set to a resolution of 0.2 eV. Quantization of the Li/C ratio was obtained by comparing the integrated areas of the C(1*s*) and Li(1*s*) peaks. To correct for differences in the photoionization cross sections of those lines, an experimentally determined value of the Li/C sensitivity ratio was employed.[34] An error assumption of ±20%, based on instrumental accuracy and experimental trials, applies to all estimates of Li atoms per molecule (x). UPS spectra were obtained using monochromatized He I radiation (21.2 eV) from a differentially pumped helium resonance lamp providing a resolution of about 0.1 eV. The work function was determined from the secondary electron cutoff. For comparison, binding energies were referenced to the vacuum level (E_{vac}), which has direct chemical significance, whereas the Fermi level (E_F) represents an instrumental artifact. Therefore, spectra are plotted according to the binding energy with respect to E_{vac}, obtained by adding the work function to the binding energy as measured with respect to the E_F.

Density of state (DOS) calculations were performed using HYPERCHEM Professional, Release 7 using a semiempirical PM3 methodology. The absolute orbital energies obtained were multiplied by a factor of 1.1, then rigidly shifted to a lower binding energy to match experimental spectra.

RESULTS AND DISCUSSION

Biphenyl and bipyridine derivatives

The UPS spectra for the pristine and lithium-intercalated BP are shown in Fig. 1. In the pristine BP spectrum, there are four main features at binding energies of 13.2, 10.9, 8.1, and 7.2 eV corresponding to photoelectron emission from the $1b_{2g}$, $2b_{3u}$, ($1b_{1g}$,$1a_u$), and $2b_{2g}$ molecular orbitals, respectively.[35] The HOMO is represented by the $2b_{2g}$ orbital and can be discerned as a shoulder at approximately 7.2 eV. Upon exposure to lithium vapor, the work function, indicated by vertical lines, decreases gradually from 3.7 eV in the pristine material to 2.6 eV in the fully intercalated film. This change is consistent with the creation of new occupied electronic states in the gap of the pristine material.[12]

The new electronic states are evident, even at low intercalation levels, in two new spectral features at the low-binding-energy side of the former HOMO, denoted A and B. Their intensity gradually increases with the intercalation level. Charge transfer from lithium and the presence of a

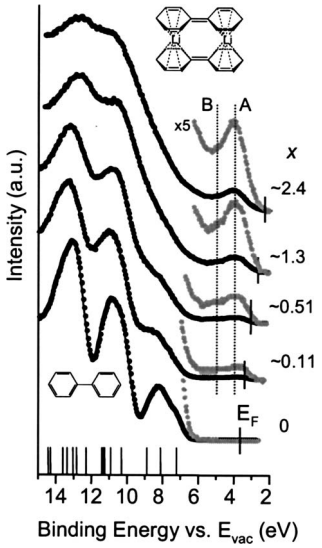

FIG. 1. The UPS spectra of BP are shown during Li intercalation. The calculated DOS of pristine BP is shown at the bottom, and the predicted structure of the intercalated compound (Ref. 46) is illustrated at the top right.

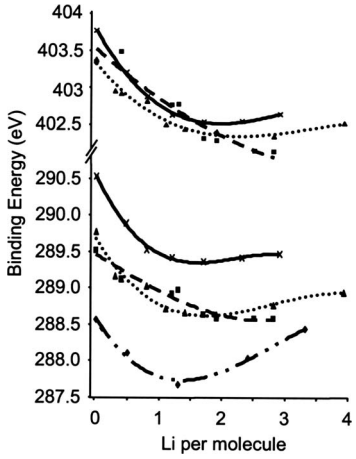

FIG. 2. Binding energy of the N(1*s*) and C(1*s*) core levels are shown for BP (♦···), 2bipy (▲··), 4bipy (■--), and 2bpmy (×—) as a function of the degree of Li intercalation.

positive counterion induce a change in the structural and electronic properties of BP from an aromatic to a quinoidal system,[36] thereby destabilizing the HOMO, resulting in a shift to the corresponding feature, B, at a binding energy of approximately 5.2 eV. Experimentally, the quinoidal state of the BP anion has been observed via shifts in C–C vibrational frequencies relative to the neutral molecule.[37] The second feature, A, at 4.0 eV, arises from photoelectron emission of the newly occupied molecular LUMO.[12,19,20,38] Thus, the splitting between A and B is about 1.2 eV.

Ramsey and co-workers have contributed a series of publications[39–42] suggesting bipolaron formation in thin biphenyl films deposited onto metallic cesium. The spectra shown in Fig. 1 are consistent with a polaronic state at low intercalation levels ($x \leqslant 0.5$), as evidenced by the spectral weight at the Fermi level.[12,13,43] At higher intercalation levels, however, peak A shifts away from the Fermi level and may indicate the formation of a bipolaronic state. The gradual manner in which the Fermi energy shifts as a function of intercalation level also provides some evidence of a transition from a polaronic to a bipolaronic state.[13,44,45]

Lischka and co-workers[19,20,46,47] have theoretically analyzed the position of intercalated lithium atoms with respect to the molecules within isolated Li-BP complexes. According to their calculations, a single lithium atom interacts through a cation-π binding configuration, where the Li counterion is approximately equidistant from the carbon atoms in one of the BP rings and positioned almost directly above the center of that ring. If two lithium atoms bind to the same BP molecule, the lithium position is shifted closer to the outer carbon atoms.[19] The most stable configuration was calculated for a sandwich-type, cation-π complex in which two BP molecules are bound cofacially with two lithium atoms, each lithium atom centered between one of the phenylene rings (shown in Fig. 1).[46]

The shift in the C(1*s*) peak toward a lower binding energy upon Li intercalation in BP (Fig. 2) indicates an increased charge density in the organic system caused by charge transfer from Li atoms to BP. At low intercalation levels ($x < 1.5$) the binding energy decreases from 288.6 to 287.7 eV. At higher intercalation levels, this trend reverses. This indicates (i) that the maximum amount of charge transferred to the organic part is achieved at about 1.5 Li atoms per molecule and (ii) that the amount of charge transferred to the aromatic system is high, possibly larger than one electron for $x=1.5$. At $x>1.5$, the shift in the C(1*s*) peak back to a higher binding energy may be attributed to a higher degree of final state screening in the Li-intercalated system. The same phenomenon has been observed previously in Li-intercalated thin films of α- and β-perylene.[11] Changes in the Li(1*s*) binding energy were negligible and within 59.1 ± 0.1 eV for all samples investigated and all values of x.

Density functional calculations[46] have shown that the amount of charge transferred per Li atom in a biphenyl film can range from 0.47 for two Li atoms bound to a single BP to 0.96 for the sandwich-type configuration described above. Our results are in agreement with configurations where each Li atom coordinates with more than one molecule. Structural effects may also play a role, as density functional calculations predict significant geometric differences between neutral and anionic radical species, particularly in the torsional angle between the two rings.[37] At high intercalation levels ($x \geqslant 3$, spectra not shown) a Fermi edge could be identified in the UPS spectra indicating the formation of a metallic overlayer.

The UPS spectrum of pristine 2bipy films [Fig. 3(a)] shows a spectral feature related to the HOMO (π_6)[48,49] at approximately 7.7 eV as a shoulder on the low-binding-energy side of that related to the lone pair orbital ($n+,n-$)[48,49] at 9.2 eV. Upon lithium intercalation, two features, denoted A′ and B′, appear at the low-binding-energy side of the HOMO in the pristine material. Shoulder B′ at 6.6 eV is related to the destabilized former HOMO, and A′ at 4.0 eV corresponds to photoelectron emission from the now partially filled LUMO, yielding a splitting between A′ and B′ of approximately 2.6 eV for the intercalated compound. Relative to BP, the larger splitting originates prima-

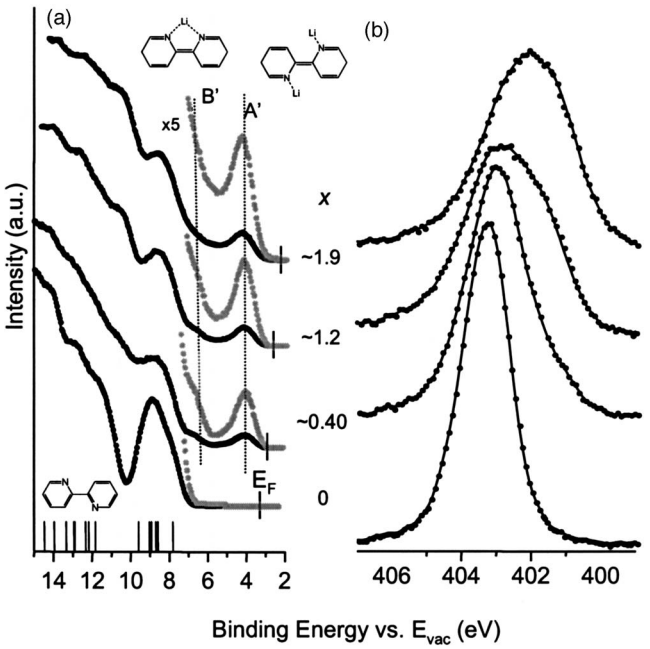

FIG. 3. The UPS (a) and the N(1*s*) core level (b) spectra of 2bipy are shown during Li intercalation. The calculated DOS of pristine 2bipy is shown at the bottom, and the predicted structure of the intercalated compound is illustrated at the top of (a), based on calculations made by Zhu *et al.* (Ref. 28).

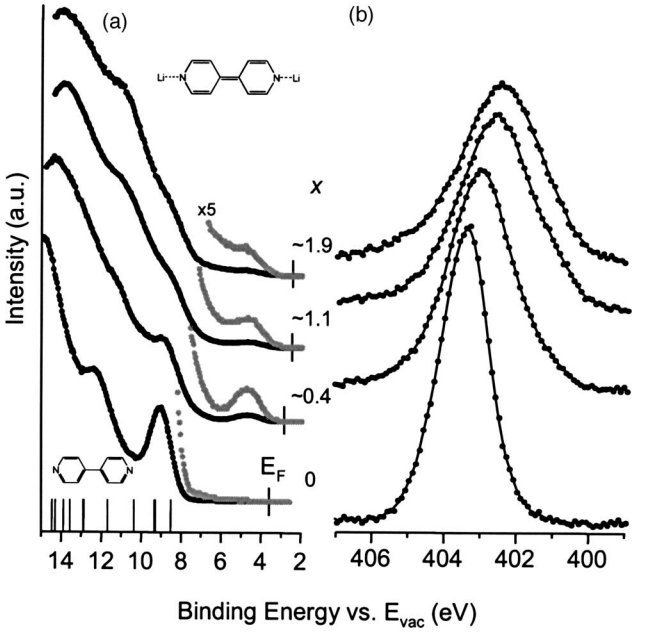

FIG. 4. The UPS (a) and the N(1*s*) core level (b) spectra of 4bipy are shown during Li intercalation. The calculated DOS of pristine 4bipy is shown at the bottom, and the predicted structure of the intercalated compound is illustrated at the top of (a), based on calculations by Zhu *et al.* (Ref. 28).

rily from differences in the magnitude of the HOMO destabilization energies: 1.8 eV in BP and 0.9 eV in 2bipy. This implies that the presence of heteroatomic nitrogen significantly stabilizes the quinoidal form of the molecular anion. Furthermore, the absence of spectral density at the Fermi level may indicate direct formation of the bipolaron state, even at low intercalation levels.

The N(1*s*) XPS spectra for 2bipy [Fig. 3(b)] show a significant chemical shift of more than 1 eV with the amount of Li intercalation, from 403.4 eV to a minimum of 402.3 eV, with a shoulder discernible on the low-binding-energy side of the main peak appearing at approximately $x=1$. However, in contrast to Li-intercalated aniline oligomers,[26] the interaction is not localized at the nitrogen atomic sites. A similar magnitude of chemical shift is observed in the C(1*s*) line from 289.8 to 288.7 eV (Fig. 2). At higher levels ($x>2$) the trend reverses and both the N(1*s*) and C(1*s*) binding energies begin to increase, although not as pronounced as for BP, indicating that the maximum amount of charge is transferred to the organic component at $x=2$.

While the most likely binding configuration in Li-intercalated BP can be represented as a sandwich-type, cation-π structure (described above), differences in electron density due to the presence of the nitrogen heteroatom warrant a different configuration for Li-2bipy. Density functional calculations by Zhu *et al.*[28] predict the binding interactions between lithium and nucleobases. Taken into account are both the possibility of cation-π binding (as in BP where the Li atom is situated approximately equidistant from each carbon atom in the ring to which it is bound) and direct cation-heteroatom binding. The latter case was found to be energetically favorable. In such a configuration, the Li atoms are bound to nitrogen atoms and held in the plane of the molecule, with bidentate interactions favored over unidentate. These results are supported in a similar work by Russo *et al.*[29] Based on these analyses, a hypothetical structure of Li-intercalated 2bipy is shown in Fig. 3. Qualitatively, this cation-heteroatom binding configuration is further supported by the lesser degree of spectral broadening in the higher binding energy, valence orbital spectra observed in Li-2bipy relative to Li-BP. In 2bipy, the Li atom interacts much less with the molecular π orbitals than in BP.

In order to study the effect of heteroatom position on the binding configuration, Li intercalation was also performed in 4,4′-bipyridine (4bipy). Figures 4(a) and 4(b) show the UPS and N(1*s*) XPS spectra of 4bipy, respectively. In the pristine film, the relatively sharp feature at 9.0 eV is comprised of the *n*-(HOMO), *n*+, π_6, π_5, and π_4 states, which are nearly degenerate.[49] Upon lithium intercalation, photoelectron emission from the newly occupied LUMO is observed by a strong peak at 4.7 eV, indicating charge transfer from Li to 4bipy. However, despite spectroscopic evidence of a quinoidal conformation in anionic 4bipy in solution, and when vacuum deposited on metallic potassium,[50] no clear feature indicating a destabilized HOMO is observed in Fig. 4(a).

The binding energy of the N(1*s*) line of 4bipy [Fig. 4(b)] decreases from 403.3 to 402.4 eV upon lithium intercalation. The peak evolution, however, is different from that observed for 2bipy. Here, the N(1*s*) line maintains its symmetry (i.e., no clear shoulder formation), broadening, and shifting with additional Li intercalation. Unlike 2bipy and BP, there is no reversal of the peak shift at higher intercalation levels (Fig. 2) in either the C(1*s*) or N(1*s*) lines. This means that the amount of charge donated to the organic component and the relative degree of charge screening remain approximately constant at intercalation levels of more than $x=1.5$. Correspondingly, with increased Li concentration, the amount of charge transferred per Li atom decreases.

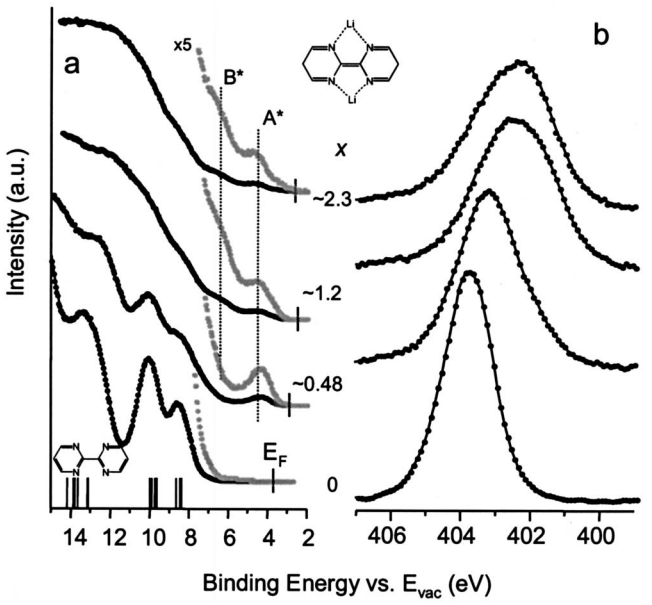

FIG. 5. The UPS (a) and the N(1*s*) core level (b) spectra of 2bpmy are shown during Li intercalation. The calculated DOS of pristine 2bpmy is shown at the bottom, and the predicted structure of the intercalated compound is illustrated at the top of (a), based on calculations by Zhu *et al.* (Ref. 28).

The absence of a clear feature corresponding to the destabilized HOMO level in Li-intercalated 4bipy may indicate a relationship between the binding configuration of the Li atom and the tendency of the host molecule to adopt an aromatic or quinoidal structure. A simplified, hypothetical structure of Li-intercalated 4bipy is shown in Fig. 4(a), with dominant cation-heteroatom binding. The rationale is the same as used for 2bipy, with the exception of intramolecular bidentate interactions, which are not possible in 4bipy. At this point, two interesting correlations can be made. As the Li atom position deviates from the cation-π configuration, shown in Fig. 1, to a heteroatom-cation configuration at the outer perimeter of the molecule, as in Fig. 4(a), (i) the splitting energy between the frontier orbitals increases (from 1.2 eV in BP to 2.6 eV in 2bipy to 4.3 eV in 4bipy) and (ii) the magnitude of the core level binding energy trend reversal at high intercalation levels ($x>1.5$) is reduced (see Fig. 2) from 0.7 eV in BP to 0.3 eV in 2bipy to no reversal in 4bipy.

The former correlation is consistent with observations made in Li- and Na-intercalated spiro-oligophenyl systems, where the size of the intercalant atom determined the optimal binding site.[44] The splitting energy between frontier orbitals was found to be smaller with a Li intercalant, where the Li atom was positioned approximately equidistant from six carbon atoms in the same aromatic ring (as in BP, Fig. 1), versus a Na intercalant, in which the counterion was situated off center with respect to the aromatic rings.

To ascertain the affect of the nitrogen/carbon ratio in these small molecules, the same Li intercalation procedure was performed on 2,2′-bipyrimidine (2bpmy), shown in Fig. 5(a). It was hypothesized that additional nitrogen in the aromatic system would have a profound effect on the Li intercalation properties, particularly on the saturation level, and the amount of charge transferred from the Li atoms. The UPS spectra of the pristine and intercalated films are shown in Fig. 5(a). In the pristine film, the peak at 8.7 eV represents the n_{A-}, n_{A+}, and $\pi_6(\pi_b)$ levels, where n_{A-} is the HOMO. The feature at 10.2 eV is derived from the n_{S+}, $\pi_5(\pi_{b+})$, $\pi_4(\pi_{a-})$, n_{S-}, and $\pi(\pi_{a+})$ electronic states.[48] As the film is exposed to Li vapor, a charge transfer from atomic Li into the LUMO occurs resulting in peak A^* observed at 4.4 eV. The destabilized HOMO becomes evident as a low-binding-energy shoulder B^* at 6.4 eV, yielding a splitting between A^* and B^* of about 2 eV. This value falls between the splitting energies obtained for BP and 2bipy suggesting, according to the above correlation, a stronger cation-π interaction than observed in 2bipy.

However, the trends observed in the core level binding energy shifts are similar to that observed for 2bipy. The N(1*s*) line [Figs. 2 and 5(b)] shifts from 403.6 to 402.4 eV, while the C(1*s*) line (Fig. 2) shifts from 290.5 eV to a minimum of 289.4 eV. The trend is reversed at higher intercalation levels ($x>2$) to roughly the same degree as observed in 2bipy.

Given the strong and local interactions between Li and N atoms, it was expected that 2bpmy would bind more Li atoms and accommodate more charge than the bipyridines owing to the larger N/C ratio. Experimentally, however, this was not observed. The saturation level of about 1.5–2 Li atoms per molecule, as indicated by the point at which additional Li atoms no longer affect the spectral features, is essentially the same for all biphenyl and bipyridyl derivatives studied.

Tetraphenylbenzene and tetrakis(2′-pyridyl)pyrazine

In order to study the effect of heteroatomic nitrogen in larger molecular systems, lithium intercalation was performed in thin films of 1,2,4,5-tetraphenylbenzene (TPB) and its heteroatomic analog, 2,3,5,6-tetrakis(2′-pyridyl)pyrazine (TPP).

The UPS spectra of TPB are shown in Fig. 6. Not surprisingly, the spectra are similar to those observed for BP (Fig. 1). A shoulder at approximately 6.8 eV is related to the HOMO. Upon Li intercalation, photoelectron emission originating from the now (partially) occupied former LUMO is evident in a peak A″ that eventually shifts to 4.0 eV at a level of about 4 Li atoms per molecule. Shoulder B″ at about 5.1 eV might be related to the destabilized HOMO, similar to the behavior observed for BP. Interestingly, the sharpness of individual features that was initially lost upon intercalation is partially restored at higher intercalation levels. This phenomenon was not observed for any of the other materials reported here and might indicate that structural homogeneity within the surface region of the film is restored. This may be due to an increased energetic barrier for phenyl group rotation in the intercalated (reduced) material relative to the neutral compound.[51]

The evolution of the C(1*s*) chemical shift for Li-TPB (Fig. 7) shows three definable regions. At low intercalation levels ($x<2$), the peak shifts towards lower binding energy as charge is transferred from Li atoms to TPB. A reversal of

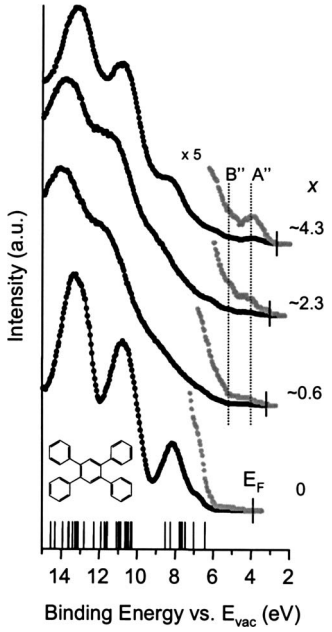

FIG. 6. The UPS spectra of TPB are shown during Li intercalation. The calculated DOS of pristine TPB is shown at the bottom.

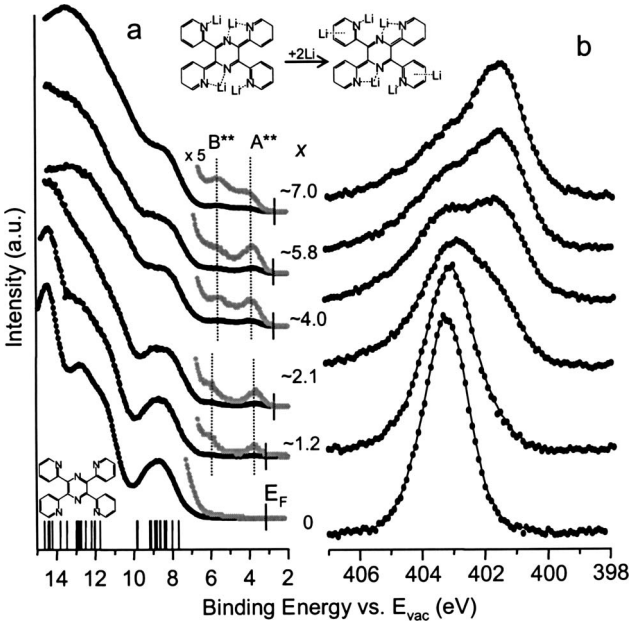

FIG. 8. The UPS (a) and the N(1*s*) core level (b) spectra of TPP are shown during Li intercalation. The calculated DOS of pristine TPP is shown at the bottom, and the predicted structure of the intercalated compound is illustrated at the top center, based on calculations by Zhu *et al.* (Ref. 28)

this trend occurs at $x\sim 2$; an unexpectedly low level since larger molecules, with a more expanded π-electron system, should be capable of increased charge storage *per molecule*.[9,34,52] Eshdat *et al.*[51] also observed a maximum charge storage of two electrons per molecule for TPB in solution using ^{13}C NMR during stepwise reduction with lithium. More highly charged species have not been reported. The similarity between the solid state reaction and the electrochemical reduction in solution demonstrate (i) that in oligophenyl systems, molecular properties dominate over solid state effects, and (ii) a trend in the molecular properties that indicates a lower energetic barrier to charge injection in smaller molecular π systems than in larger ones if the amount of charge is evaluated *per carbon atom*.[9,52]

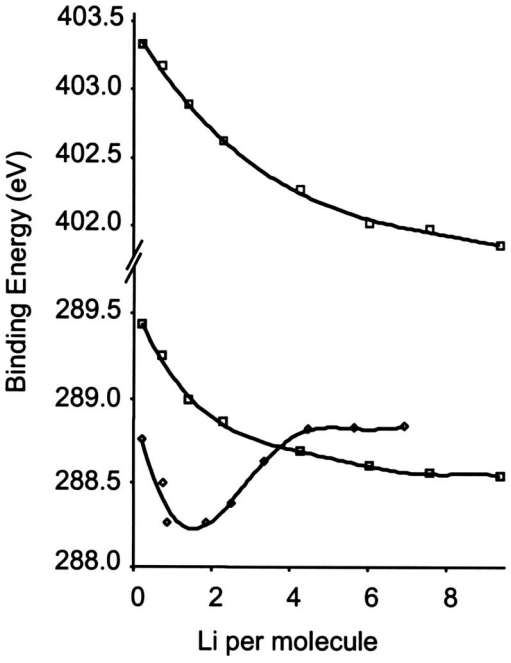

FIG. 7. Binding energy of the N(1*s*) and C(1*s*) core levels are shown for TPB (◇) and TPP (□) as a function of the degree of Li intercalation.

As observed in BP, 2bipy, and 2bpmy, at intermediate intercalation levels ($x=2-4$) the reversal of the core level binding energy trend indicates that a lower amount of charge is transferred to the organic component per Li atom. This is likely accompanied by a major change in the Li-molecule bonding configuration, as the film accommodates excess Li atoms. At high intercalation levels ($x>4$) this change is completed and the binding energy becomes stable with increasing Li concentration.

Figure 8(a) shows the UPS spectra of TPP, the nitrogenous analog to TPB. In the pristine film, a very broad feature centered at 8.6 eV is related to the HOMO. Upon Li intercalation, a peak corresponding to emission from the now (partially) occupied former LUMO becomes evident at 3.8 eV (A^{**}). Destabilization of the HOMO forms shoulder B^{**} at 6.0 eV at low intercalation levels ($x<4$) which shifts to 5.4 eV at higher intercalation levels ($x>4$). This change corresponds to a 0.6 eV decrease of the splitting between A^{**} and B^{**} with the amount of Li intercalated, a trend not observed elsewhere in this work.

Changes to the N(1*s*) line [Figs. 7 and 8(b)] with Li deposition are also more pronounced than with the smaller model systems, shifting from 403.3 eV in the pristine film to 401.8 eV in the fully intercalated film. In Fig. 8(b), a clear shoulder at 401.4 eV begins to develop at low intercalation levels, corresponding to nitrogen sites which have reacted with Li atoms. The shoulder evolves into the dominant spectral feature at about $x=7$. In Fig. 7, it can be seen that there is a pronounced change in the peak shift dynamics at about $x=4$, above which binding energy shifts are more gradual.

This change, in addition to the change of the splitting between A^{**} and B^{**} occurring at about $x=4$, suggests two different binding scenarios for Li in TPP.

From these data, we propose that the first four Li atoms to be intercalated are bound directly to nitrogen atoms, in either a uni- or bidentate cation-heteroatom configuration, as suggested for the bipyridine films. At higher intercalation levels, additional Li still interacts closely with TPP, as evidenced by continual changes in the UPS spectra up to $x=7$. The observed decrease in splitting energy above $x=4$ suggests that these interactions consist of a higher degree of cation-π binding (as in BP), discussed above.

However, the additional Li concentration has a relatively small effect on the core level binding energies of both carbon and nitrogen atoms (see Fig. 7), and the amount of charge transferred to the organic component saturates. Since the charge transfer per Li atom is smaller than at lower intercalation levels, the bonds between Li and the organic component are weaker, requiring less energy to reverse the intercalation process.

Thus, these results have important implications for Li-ion battery development. Relative to TPB, the nitrogen heteroatoms in TPP increase the total charge storage ability of the material by a factor of 3, from about two to possibly up to six-charges per molecule. The latter few charges are only loosely bound, facilitating easier deintercalation. Additionally, in contrast to the oligophenyl systems,[9] larger nitrogen-substituted systems accommodate about the same amount of charge per atom as smaller ones.

CONCLUSIONS

The stepwise intercalation of lithium atoms in thin molecular films of biphenyl, selected bipyridine derivatives, and larger, branched oligomer analogs was performed in an ultrahigh vacuum environment. A structural change from an aromatic to a quinoidal form upon intercalation was observed as evidenced by the appearance of a spectral feature related to a destabilized HOMO level. The position of this feature and the splitting energy between gap states in the intercalated material were found to be dependent on the substitution position of nitrogen in the aromatic network.

In smaller systems, i.e., biphenyl and bipyridine derivatives, the presence of the nitrogen heteroatom does not significantly affect the charge storage capacity or reversibility of lithium binding. In all cases, the maximum amount of charge transfer was obtained at a level of approximately 1.5–2 Li atoms per molecule.

In larger, branched derivatives, however, the presence of heteroatomic nitrogen had a more profound effect. The amount of charge storage may be increased by a factor of 3 for TPP relative to TPB. In addition, a different binding configuration was observed for the first and last few Li atoms bound to TPP. The first few Li atoms intercalated are most likely bound in a direct cation-heteroatom configuration. Subsequent Li atoms are bound to TPP by cation-π interactions. The latter interactions are relatively weaker, implying a higher degree of reversibility at this stage in the intercalation process. In contrast to oligophenyls,[9] where molecular properties dominate over solid state effects, larger nitrogen-substituted molecular systems accommodate the same charge, on a per atom basis, as smaller analogs.

ACKNOWLEDGMENTS

Dr. Henri Doucet and Isabelle Kondolff are gratefully acknowledged for providing minute amounts of TPB. This work is sponsored by the Swedish Science Research Council (VR) under Contract Nos. 12252003 and 12252020. Research in general at Linköping is additionally supported by the Swedish Foundation for Strategic Research through the Center for Advanced Molecular Materials (CAMM), the EU growth project for a Molecular Approach to Carbon based Materials for Energy Storage (MAC-MES), the Center for Organic Electronics (COE), the Commission of the European Union through the Integrated Project NAIMO (No. NMP4-CT-2004-500355), as well as through contracts with DuPont Corporation, USA and Merck Chemicals, UK.

[1] K. Sato, M. Noguchi, A. Demachi, N. Oki, and M. Endo, Science **264**, 556 (1994).
[2] H. Shimoda, B. Gao, X. P. Tang, A. Kleinhammes, L. Fleming, Y. Wu, and O. Zhou, Physica B **323**, 133 (2002).
[3] H. Ago, K. Nagata, K. Yoshizawa, K. Tanaka, and T. Yamabe, Bull. Chem. Soc. Jpn. **70**, 1717 (1997).
[4] H. Ago, M. Kato, K. Yahara, K. Yoshizawa, K. Tanaka, and T. Yamabe, J. Electrochem. Soc. **146**, 1262 (1999).
[5] D. A. Morton-Blake, J. Corish, and F. Beniere, Theor. Chim. Acta **68**, 389 (1985).
[6] L. G. Scanlon and G. Sandi, J. Power Sources **82**, 176 (1999).
[7] G. Brancolini and F. Negri, Carbon **42**, 1001 (2004).
[8] M. Nakadaira, R. Saito, T. Kimura, G. Dresselhaus, and M. S. Dresselhaus, J. Mater. Res. **12**, 1367 (1997).
[9] R. Friedlein, X. Crispin, and W. R. Salaneck, J. Power Sources **129**, 29 (2004).
[10] J. Schnadt, P. A. Bruhwiler, N. Martensson, A. Lassesson, F. Rohmund, and E. E. B. Campbell, Phys. Rev. B **62**, 4253 (2000).
[11] R. Friedlein, X. Crispin, C. Suess, M. Pickholz, and W. R. Salaneck, J. Chem. Phys. **121**, 2239 (2004).
[12] P. Dannetun, M. Logdlund, M. Fahlman, C. Fauquet, D. Beljonne, J. L. Bredas, H. Bassler, and W. R. Salaneck, Synth. Met. **67**, 81 (1994).
[13] G. Iucci, K. Xing, M. Logdlund, and M. Fahlman, Chem. Phys. Lett. **244**, 139 (1995).
[14] W. R. Salaneck, H. R. Thomas, C. B. Duke, A. Paton, E. W. Plummer, A. J. Heeger, and A. G. MacDiarmid, J. Chem. Phys. **71**, 2044 (1979).
[15] Y. H. Kim, D. Spiegel, S. Hotta, and A. J. Heeger, Phys. Rev. B **38**, 5490 (1988).
[16] J. L. Bredas and G. B. Street, Acc. Chem. Res. **18**, 309 (1985).
[17] J. Cornil, D. Beljonne, and J. L. Bredas, J. Chem. Phys. **103**, 842 (1995).
[18] W. R. Salaneck, R. H. Friend, and J. L. Bredas, Phys. Rep. **319**, 232 (1999).
[19] S. Irle and H. Lischka, J. Chem. Phys. **103**, 1508 (1995).
[20] S. Irle and H. Lischka, J. Mol. Struct.: THEOCHEM **364**, 15 (1996).
[21] S. Ito, T. Murata, M. Hasegawa, Y. Bito, and Y. Toyoguchi, J. Power Sources **68**, 245 (1997).
[22] Y. P. Wu, S. Fang, and Y. Jiang, Solid State Ionics **120**, 117 (1999).
[23] Y. P. Wu, C. Y. Jiang, C. R. Wan, S. B. Fang, and Y. Y. Jiang, J. Appl. Polym. Sci. **77**, 1735 (2000).
[24] Y. P. Wu, E. Rahm, and R. Holze, Electrochim. Acta **47**, 3491 (2002).
[25] W. J. Weydanz, B. M. Way, T. van Buuren, and J. R. Dahn, J. Electrochem. Soc. **141**, 900 (1994).
[26] I. Kuritka, F. Negri, G. Brancolini, C. Suess, W. R. Salaneck, and R. Friedlein, (unpublished).
[27] Z.-X. Wang, T. K. Manojkumar, C. Wannere, and P. von Rague Schleyer, Org. Lett. **3**, 1249 (2001).
[28] W. Zhu, X. Luo, C. M. Puah, X. Tan, J. Shen, J. Gu, K. Chen, and H. Jiang, J. Phys. Chem. A **108**, 4008 (2004).
[29] N. Russo, M. Toscano, and A. Grand, J. Phys. Chem. B **105**, 4735 (2001).

[30] T. Hasegawa, T. Suzuki, S. R. Mukai, and H. Tamon, Carbon **42**, 2195 (2004).
[31] F. Berthiol, I. Kondolff, H. Doucet, and M. Santelli, J. Organomet. Chem. **689**, 2786 (2004).
[32] H. A. Goodwin and F. Lions, J. Am. Chem. Soc. **81**, 6415 (1959).
[33] W. R. Salaneck, R. Bergman, J. E. Sundgren, A. Rockett, T. Motooka, and J. E. Greene, Surf. Sci. **198**, 461 (1988).
[34] R. Friedlein, X. Crispin, M. Pickholz, M. Keil, S. Stafstrom, and W. R. Salaneck, Chem. Phys. Lett. **354**, 389 (2002).
[35] M. Rubio, M. Merchan, E. Orti, and B. O. Roos, J. Phys. Chem. **99**, 14980 (1995).
[36] A. J. Heeger, S. Kivelson, J. R. Schrieffer, and W.-P. Su, Rev. Mod. Phys. **60**, 781 (1988).
[37] K. Furuya, H. Torii, Y. Furukawa, and M. Tasumi, J. Mol. Struct.: THEOCHEM **424**, 225 (1998).
[38] N. Koch, A. Rajagopal, E. Zojer, J. Ghijsen, X. Crispin, G. Pourtois, J. L. Bredas, R. L. Johnson, J. J. Pireaux, and G. Leising, Surf. Sci. **454**, 1000 (2000).
[39] M. G. Ramsey, F. P. Netzer, D. Steinmuller, D. Steinmullernethl, and D. R. Lloyd, J. Chem. Phys. **97**, 4489 (1992).
[40] F. P. Netzer, M. G. Ramsey, and D. Steinmuller, Synth. Met. **41**, 1343 (1991).
[41] M. G. Ramsey, D. Steinmuller, and F. P. Netzer, Phys. Rev. B **42**, 5902 (1990).
[42] M. G. Ramsey, D. Steinmuller, and F. P. Netzer, J. Chem. Phys. **92**, 6210 (1990).
[43] Y. Onodera, Phys. Rev. B **30**, 775 (1984).
[44] A. Crispin, X. Crispin, M. Fahlman *et al.*, J. Chem. Phys. **116**, 8159 (2002).
[45] G. Greczynski, M. Fahlman, and W. R. Salaneck, J. Chem. Phys. **113**, 2407 (2000).
[46] S. Irle, H. Lischka, K. Eichkorn, and R. Ahlrichs, Chem. Phys. Lett. **257**, 592 (1996).
[47] S. Irle and H. Lischka, J. Chem. Phys. **107**, 3021 (1997).
[48] V. Barone, F. Lelj, C. Cauletti, M. N. Piancastelli, and N. Russo, Mol. Phys. **49**, 599 (1983).
[49] V. Barone, F. Lelj, L. Commisso, N. Russo, C. Cauletti, and M. N. Piancastelli, Chem. Phys. **96**, 435 (1985).
[50] H. Kihara and Y. Gondo, J. Raman Spectrosc. **17**, 263 (1986).
[51] L. Eshdat, A. Ayalon, R. Beust, R. Shenhar, and M. Rabinovitz, J. Am. Chem. Soc. **122**, 12637 (2000).
[52] R. Friedlein, X. Crispin, and W. R. Salaneck, Rec. Res. Dev. Chem. Phys. **4**, 457 (2003).